EARTHQUAKE ENGINEERING AND STRUCTURAL DYNAMICS, VOL. 25, 585-597 (1996)

ACTIVE TENDON CONTROL OF CABLE-STAYED BRIDGES

Y. ACHKIRE AND A. PREUMONT

Service des Constructions, Mecaniques et Robotique, Université Libre de Bruxelles, 50 Av. F.D. Roosevelt, B-1050 Brussels, CP 165, Belgium

SUMMARY

This paper considers the active vibration control of cables and cable/structure systems with an active tendon controlling the axial displacement of the cable anchor point. It is demonstrated that a force feedback based on a collocated force sensor measuring the tension in the cable is feasible and that this control configuration can be associated with control laws with guaranteed stability properties. Experimental results are presented on a cable with small sag and on a cable/structure system. They show that the control algorithm can provide the structure with several percent of active damping and that the parametric resonance does not occur when the natural frequency of the structure is twice that of the cable.

KEY WORDS: cable-stayed bridges; cable dynamics; vibration; control

1. INTRODUCTION

Cable vibration has become a major issue in the design of cable stayed bridges, because their ever increasing span makes them more sensitive to flutter instability as well as to wind and traffic induced vibrations. The problem is difficult because of the highly non-linear behaviour of cables with sag: the cable excites the girder through the time varying tension in the cable and the girder excites the cable through linear coupling (inertia) and quadratic coupling terms. The latter may produce parametric excitation if some tuning conditions are satisfied.[1] Passive damping augmentation techniques do exist,[2] but active techniques are considered for future applications. The application of active tendons to flutter control has been considered by Yang.[3,4] Their application to active damping has been studied by Fujino and co-workers. They demonstrated that the first global vertical mode of the bridge can be damped with a linear feedback of the girder velocity on the active tendon displacement[5] (Figure 1(a)). In-plane (vertical) local cable vibrations can be controlled by sag induced forces (Figure 1(b)). It has been shown[6] that sag induced control is very efficient for the first in-plane mode, even for very small values of the sag to span ratio ($< 0{\cdot}5$ per cent).

Sag induced forces do not affect the out-of-plane local vibration of the cable which behaves like a taut string. Chen[7] showed on a string that the out-of-plane vibration can also be controlled by the longitudinal motion of the support at a frequency equal to twice the frequency of the transverse vibration of the string, making a positive use of the parametric excitation. This stiffness control algorithm has been tested by Fujino and co-workers[8] on a cable-structure system (Figure 1(c)). Experimental results reveal that instability can occur when the cable/structure interaction is large. This situation arises when the cable mass is significant compared to that of the girder or when the structure natural frequency is close to twice that of the cable, causing the time varying tension to resonate with the structure.

The foregoing control strategies for the global vertical mode as well as the local in-plane cable mode are prone to spillover: Control spillover arises from the control variable u exciting the higher order modes in addition to the targeted one; observation spillover results from the contamination of the sensor signal by contributions from the higher order modes. It is well known that when both control and observation spillover exist, they can result in spillover instability.[9] Spillover is mainly associated with the use of non-collocated actuator and sensor; this study proposes an alternative control strategy based on a force sensor collocated with the active tendon.

CCC 0098-8847/96/060585-13

Received 9 September 1995
Revised 18 January 1996

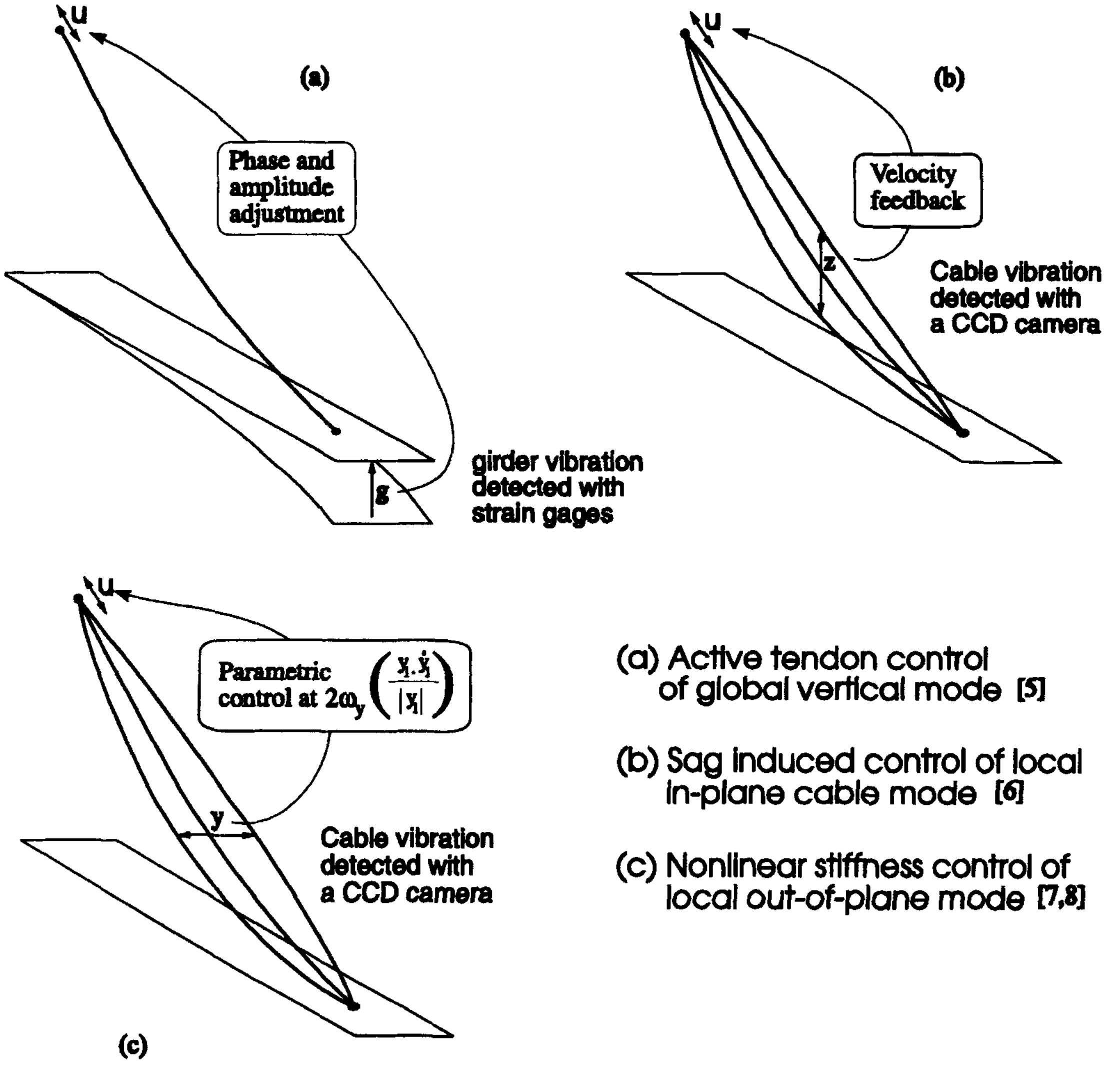

Figure 1. Existing control strategies

2. ENERGY ABSORBING CONTROL

It is widely accepted that the active damping of linear structures is much simplified if one uses collocated actuator and sensor pairs.[10] This is because the poles and zeros alternate near the imaginary axis. For such configurations, a wide class of controllers can be developed using positivity concepts.[11]

For non-linear structures, the use of collocated actuator–sensor pairs is still quite attractive, because it is possible to develop control schemes which are guaranteed to be energy absorbing, at least when we assume that the actuator and sensor dynamics are perfect. First, consider the configuration of Figure 2(a): the actuator produces a point force and the collocated sensor measures the velocity. The power flow from the control system $W = F\dot{u}$. Any control law rendering W negative will be stabilizing, because if we take the total energy E (potential + kinetics) of the vibrating structure as a Liapunov function, we have $\dot{E} = W$ (assuming no structural damping). $W < 0$ can be achieved by the feedback law,

$$F = -g\dot{u} \Rightarrow W = -g\dot{u}^2 \quad (g > 0) \tag{1}$$

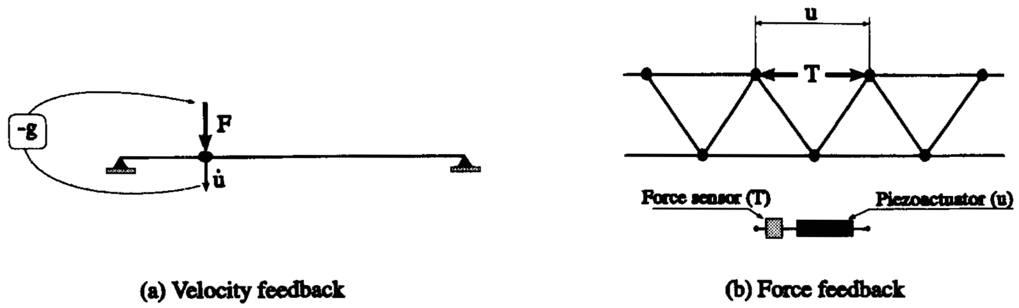

Figure 2. Energy absorbing control

This well known scheme is called *Direct Velocity Feedback*; it may not always work in practice because of actuator and sensor dynamics. A non-linear alternative feedback law is,

$$F = -F_0 \operatorname{sign}(\dot{u}) \Rightarrow W = -F_0|\dot{u}| \quad (F_0 > 0) \tag{2}$$

This 'bang-bang' control produces a faster decay, but it can lead to chattering near the equilibrium.

Next, consider the dual situation (Figure 2(b)) where the actuator controls the relative position u of two points inside the structure (e.g. piezoelectric linear actuator) and the sensor output is the force T in the active member (T is collocated with u).

As before, $\dot{E} = W = -T\dot{u}$ and it is readily verified that the *positive Integral Force Feedback*,

$$u = g\int T\,\mathrm{d}t \Rightarrow W = -gT^2 \quad (g > 0) \tag{3}$$

produces an energy absorbing control. Integral force feedback on piezoelectric actuators has already been applied successfully to the control of truss structures.[12]

From the foregoing discussion, we can anticipate that the integral force feedback will be effective in damping the global vertical mode of the bridge as well as the local in-plane mode of the cable. Moreover, this will be achieved without threat of spillover instability, provided that the actuator and sensor dynamics are good enough. Force feedback cannot be used for damping the out-of-plane modes, because these modes are not observable from the force sensor. The in-plane vibration of a cable with small sag is considered in the next section.

3. CABLE VIBRATION

3.1. *Experimental set-up*

Figure 3(a) shows the test structure and its main components. The cable is a 2 m long stainless steel wire of 0·196 mm^2 cross-section, provided with additional lumped masses at regular intervals, in order to achieve a representative value of the cable weight to tension ratio. The mass per unit length is 0·057 kg/m and the static tension in the cable is between 25 N and 50 N (a known weight is used to adjust the initial tension in the cable, prior to fixing the cable to the anchor point). For $T_0 = 25$ N, the sag to span ratio is 0·5 percent and the first in-plane frequency $f_1 = 5{\cdot}7$ Hz. One end of the cable is fixed to a lever system which is used to amplify the motion of the active element (Figure 3(b)). The active member consists of a linear piezoelectric actuator collocated with a force sensor. Because of the high-pass filter behaviour of the piezoelectric force sensor, it measures only the dynamic component of the tension in the cable. The amplification of the lever system is 3·4, corresponding to a maximum axial displacement of 150 μm for the moving support. The controller is implemented digitally, on a DSP board.

Figure 4 shows the transfer function between the voltage applied to the piezotranslator and the force signal. One notices the alternating pattern of poles and zeros, which is typical of collocated systems.[10] Only

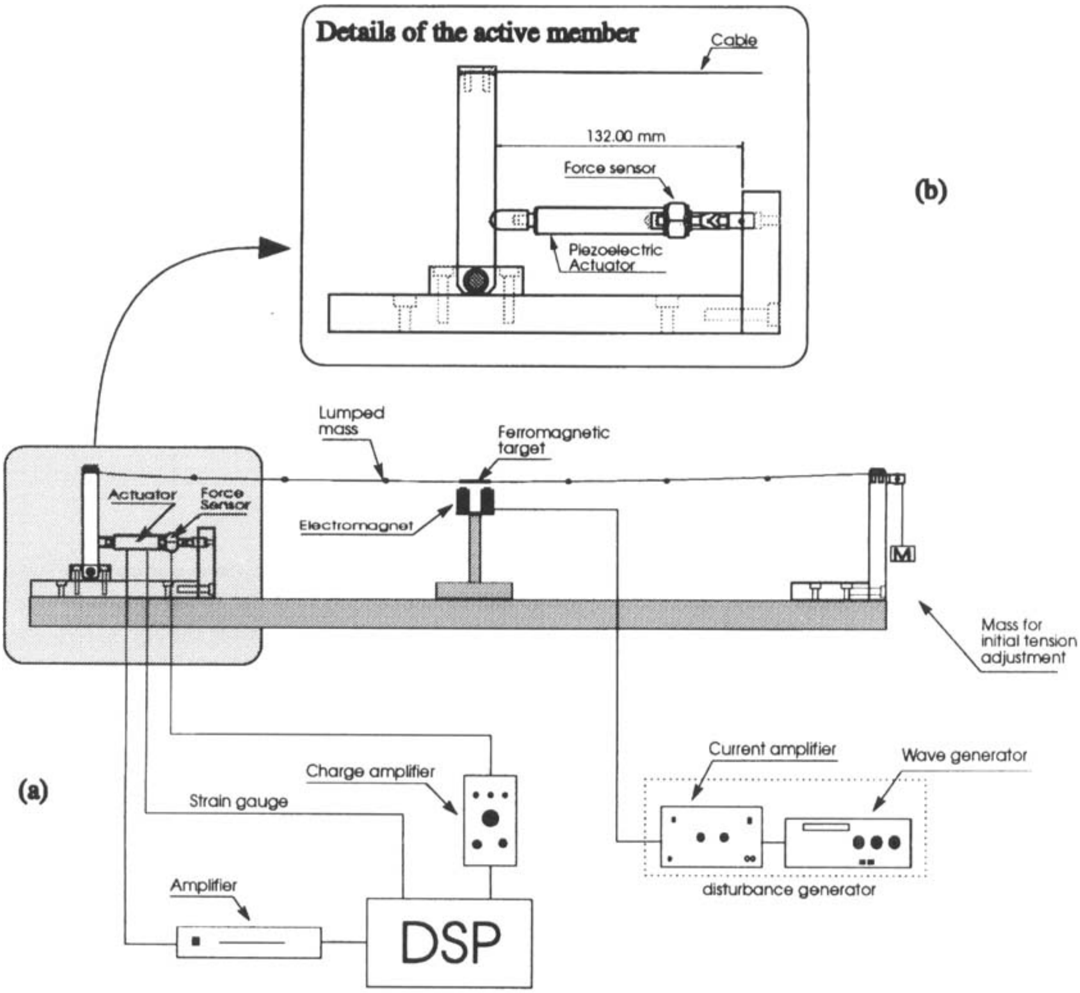

Figure 3. Cable system experimental set-up

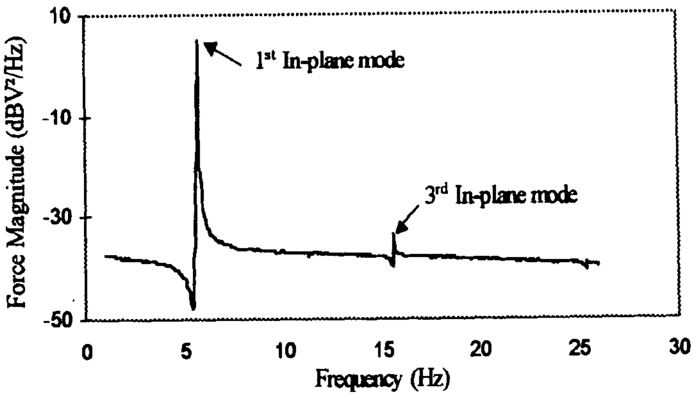

Figure 4. Experimental transfer function of the cable system

the modes of odd numbers appear in the transfer function, because the modes with even numbers are neither observable from the force sensor nor controllable from the piezotranslator.

3.2. Governing equations

The equations governing the motion, expressed in modal coordinates are as follows[5]:

Out-of-plane:

$$m_{yn}(\ddot{y}_n + 2\xi_{yn}\omega_{yn}\dot{y}_n + \omega_y^2 y_n) + \overbrace{\sum_k \nu_{nk} y_n (y_k^2 + z_k^2)}^{\text{Cable stretching}} + \sum_k 2\beta_{nk} y_n z_k + \overbrace{R_n u y_n}^{\text{Active stiffness variation}} = F_{yn} \tag{4}$$

In-plane:

$$m_{zn}(\ddot{z}_n + 2\xi_{zn}\omega_{zn}\dot{z}_n + \omega_{zn}^2 z_n) + \sum_k \nu_{nk} z_n (y_k^2 + z_k^2) + \sum_k 2\beta_{nk} z_n z_k + R_n u z_n + \underbrace{\sum_k \beta_{kn}(y_k^2 + z_k^2)}_{\text{Cable sag}} - \underbrace{\alpha_n \frac{\mathrm{d}^2 u}{\mathrm{d}t^2}}_{\text{Active sag induced force}} = F_{zn} \tag{5}$$

Tension in the cable:

$$T = \overbrace{h_u u}^{\text{Feedthrough}} + \overbrace{\sum_n h_{2n}(y_n^2 + z_n^2)}^{\text{Cable stretching}} + \overbrace{\sum_n h_{1n} z_n}^{\text{Cable sag}} \tag{6}$$

where y_n and z_n refer to the modal amplitudes of the in-plane and out-of-plane modes respectively, and u represents the axial motion of the support. The analytical form of the coefficients can be found in Reference 5. The physical meaning of the various terms is indicated in the equations. Notice that:

(i) The active sag induced force appears only in the equations governing the in-plane motion. In addition, $\alpha_n = 0$ and $h_{1n} = 0$ if n is even.
(ii) The out-of-plane modes affect the tension in the cable only with the quadratic term (corresponding to cable stretching), while the in-plane modes have a linear influence on T.

3.3. Control law

The proposed control law is the (positive) integral force feedback (*IFF*):

$$u(t) = g \int_0^t T(\tau)\,\mathrm{d}\tau \tag{7}$$

An energy analysis is conducted to evaluate the control efficiency.[8] For simplicity, let us assume that the in-plane transverse vibration with active control, z_n, is harmonic with frequency $\hat{\omega}_{zn}$ which is close to the undamped natural frequency, $\hat{\omega}_{zn} \approx \omega_{zn}$,

$$z_n = a_{zn} \cos \omega_{zn} t \tag{8}$$

We define the energy dissipation as the integral over one cycle, $\tau_n = 2\pi/\omega_{zn}$, of the product of the generalized velocity and the generalized damping force. For a linear oscillator,

$$\ddot{z}_n + 2\xi_{zn}\omega_{zn}\dot{z}_n + \omega_{zn}^2 z_n = 0 \tag{9}$$

the energy dissipation due to inherent damping can be written as,

$$E_p(2\xi_{zn}\omega_{zn}\dot{z}_n) = \int_0^{\tau_n} -(2\xi_{zn}\omega_{zn}\dot{z}_n)\dot{z}_n\,\mathrm{d}t = -2\pi\xi_{zn}(a_{zn}\omega_{zn})^2 \tag{10}$$

Returning to the cable system, the differential motion of the cable support $u(t)$ creates two basic effects as seen in equations (4) and (5):

(i) *Active sag induced force* ($\alpha_n \ddot{u}$): This term is due to the presence of sag in the cable, and exists for the in-plane symmetric modes only.
(ii) *Active stiffness variation*: $R_n u y_n$ and $R_n u z_n$.

The energy dissipation due to the sag induced force with the *IFF* controller is,

$$E_p(-\alpha_n\ddot{u}) = \int_0^{\tau_n} -(-\alpha_n\ddot{u})\dot{z}_n\,\mathrm{d}t = \int_0^{\tau_n} -(-\alpha_n g\dot{T})\dot{z}_n\,\mathrm{d}t \tag{11}$$

Upon substituting T from equation (6) and introducing $y_n = 0$ and $z_n = a_{zn}\cos\omega_{zn}t$, we find, after some algebra,

$$E_p(-\alpha_n\ddot{u}) = -2\pi\xi_{zn}(\alpha_{zn}\omega_{zn})^2 \frac{2}{(n\pi)^4}\lambda^2[1 + (-1)^{n+1}]\frac{gh_u/\omega_{zn}}{1 + (gh_u/\omega_{zn})^2} \tag{12}$$

with,

$$\lambda^2 = \frac{64}{\varepsilon_0}\left(\frac{d}{l}\right)^2 \tag{13}$$

where ε_0 is the static strain of the cable, d is the sag at midspan and l is the length. λ^2 is known as the *Irvine* parameter.[13]

The equivalent linear damping ξ_{zn}^{ai} is obtained by comparing equation (12) to the corresponding equation for the linear oscillator (10); we get

$$\xi_{zn}^{ai} = \frac{2}{(n\pi)^4}\lambda^2[1 + (-1)^{n+1}]\frac{gh_u/\omega_{zn}}{1 + (gh_u/\omega_{zn})^2} \tag{14}$$

Similarly, the energy dissipation due to active stiffness control is,

$$E_p(R_n u z_n) = \int_0^{\tau_n} -(R_n u z_n)\dot{z}_n\,\mathrm{d}t \tag{15}$$

Following the same procedure, we find, after some algebra

$$E_p(R_n u z_n) = -2\pi\xi_{zn}(a_{zn}\omega_{zn})^2 \frac{1}{8}\frac{1}{\varepsilon_0}\left(\frac{a_{zn}}{l}\right)^2 \frac{gh_u/2\omega_{zn}}{1 + (gh_u/2\omega_{zn})^2} \tag{16}$$

By comparing to equation (10), the equivalent linear damping ξ_{zn}^{as} due to the active stiffness force is,

$$\xi_{zn}^{as} = \frac{1}{8}\frac{1}{\varepsilon_0}\left(\frac{a_{zn}}{l}\right)^2 \frac{gh_u/2\omega_{zn}}{1 + (gh_u/2\omega_{zn})^2} \tag{17}$$

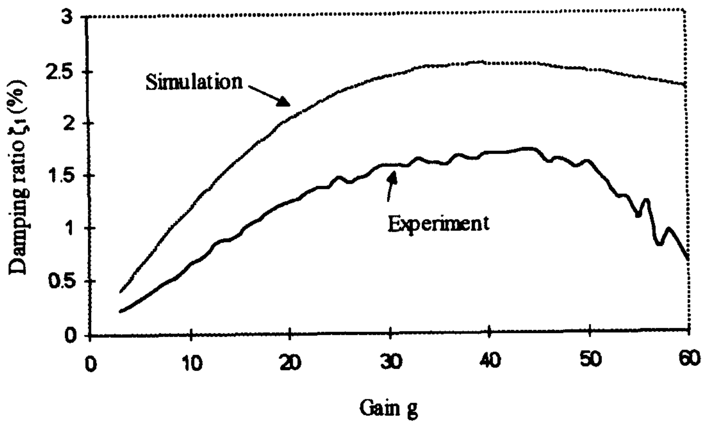

Figure 5. Active damping with *Integral Force Feedback* ($d/l = 0{\cdot}5\%$)

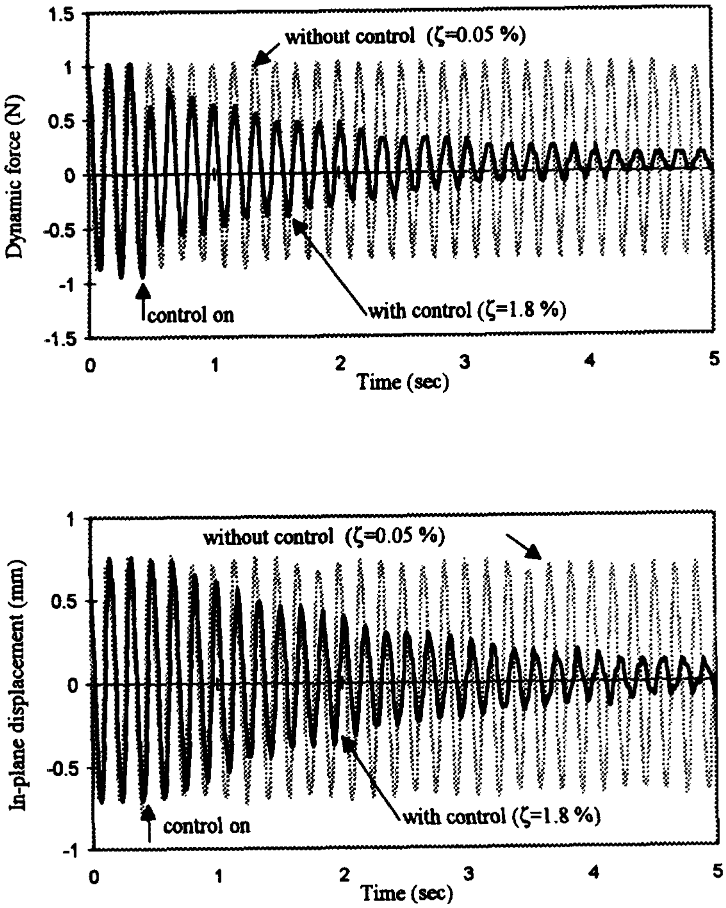

Figure 6. Free oscillations with *Integral Force Feedback*

ξ_{zn}^{as} depends on the square of the amplitude α_{zn}. For small amplitudes, it is dominated by the sag induced damping,

$$\xi_{zn}^{ai} \gg \xi_{zn}^{as} \tag{18}$$

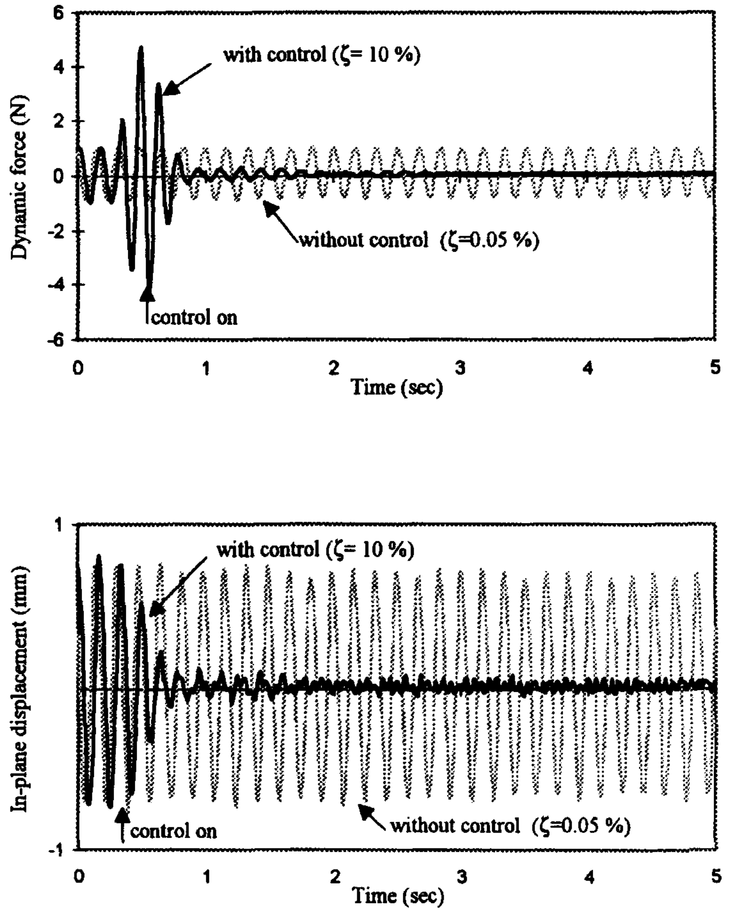

Figure 7. Free oscillations with a *P minus I* controller

The maximum value of the sag induced damping ξ_{zn}^{ai} is obtained for $g = h_u/\omega_{zn}$,

$$\xi_{zn}^{ai} = \frac{1}{(n\pi)^4} \lambda^4 [1 + (-1)^{n+1}] \tag{19}$$

3.4. *Experimental results*

In the practical implementation of the integral force feedback, only the dynamic component of the tension in the cable is considered. In addition to that, a forgetting factor is applied to prevent saturation. Figure 5 compares the numerical and experimental values of ξ_1. The descrepancy between the simulations and the experiments is attributed to errors in the feedthrough coefficient. Note that the drop of the active damping coefficient for large gains is observed experimentally. Note also that the experimental values of ξ_1 are at least as good as other previously published results[6] for comparable values of d/l. The present control law, however, has the advantage that it is not subject to spillover. Figure 6 shows experimental results for the tension in the cable and the cable displacement during the free response from non-zero initial conditions, with and without control. The sudden change in the cable tension when the control is switched on is due to the feedthrough component in equation (6).

Various experiments have been conducted with other control laws; Figure 7 shows the time response obtained with a *P minus I* controller (combined with a low pass filter with cut-off frequency

near $\omega_0 = 100$ Hz). Although a very large damping ratio can be achieved for the first mode ($\xi_1 > 10$ per cent!), this control law may be destabilizing for higher modes in the experimental set-up; it is not recommanded because it is violently unstable when the cable is connected to a flexible structure as discussed below.

4. CABLE-STRUCTURE SYSTEM

4.1. Experimental set-up

In order to test the control strategy for a cable-structure system, the mock-up has been modified in such a way that one end of the cable is connected to a spring–mass system with a tunable natural frequency (Figure 8). The modified experimental set-up is represented in Figure 9; a shaker and an accelerometer are attached to the spring–mass system to evaluate the performance of the control system.

4.2. Governing equations

Because of the addition of the spring–mass system, the governing equations (4)–(6) are changed into,

Out-of-plane:

$$m_{yn}(\ddot{y}_n + 2\xi_{yn}\omega_{yn}\dot{y}_n + \omega_y^2 y_n) + \overbrace{\sum_k \nu_{nk} y_n (y_k^2 + z_k^2)}^{\text{Cable stretching}} + \overbrace{\sum_k 2\beta_{nk} y_n z_k}^{\text{Cable sag}} - \overbrace{R_n q y_n}^{\text{Parametric Excitation}} + \overbrace{R_n u y_n}^{\text{Active stiffness variation}} = F_{yn} \quad (20)$$

In-plane:

$$m_{zn}(\ddot{z}_n + 2\xi_{zn}\omega_{zn}\dot{z}_n + \omega_{zn}^2 z_n) + \sum_k \nu_{nk} z_n (y_k^2 + z_k^2) + \sum_k 2\beta_{nk} z_n z_k - R_n q z_n + R_n u z_n$$
$$+ \sum_k \beta_{kn}(y_k^2 + z_k^2) + \underbrace{\alpha_n \ddot{q}}_{\text{Inertia force}} - \underbrace{\alpha_n \ddot{u}}_{\text{Active sag induced force}} = F_{zn} \quad (21)$$

Structure:

$$M(\ddot{q} + 2\xi_q\omega_q\dot{q} + \omega_q^2 q) + h_u q - h_u u - \sum_n h_{2n}(y_n^2 + z_n^2) - \sum_n h_{1n} z_n = F_q \quad (22)$$

Cable tension:

$$T = \overbrace{\underbrace{h_u u}_{\text{Feedthrough}} - h_u q + \sum_n h_{2n}(y_n^2 + z_n^2)}^{\text{Cable stretching}} + \overbrace{\sum_n h_{1n} z_n}^{\text{Cable sage}} \quad (23)$$

where q is the axial displacement of the structure at the connection with the cable and $\omega_q^2 = K/M$. The other notations are identical to those used for the cable. Figure 10 compares the transfer functions predicted by simulations to the experiments.

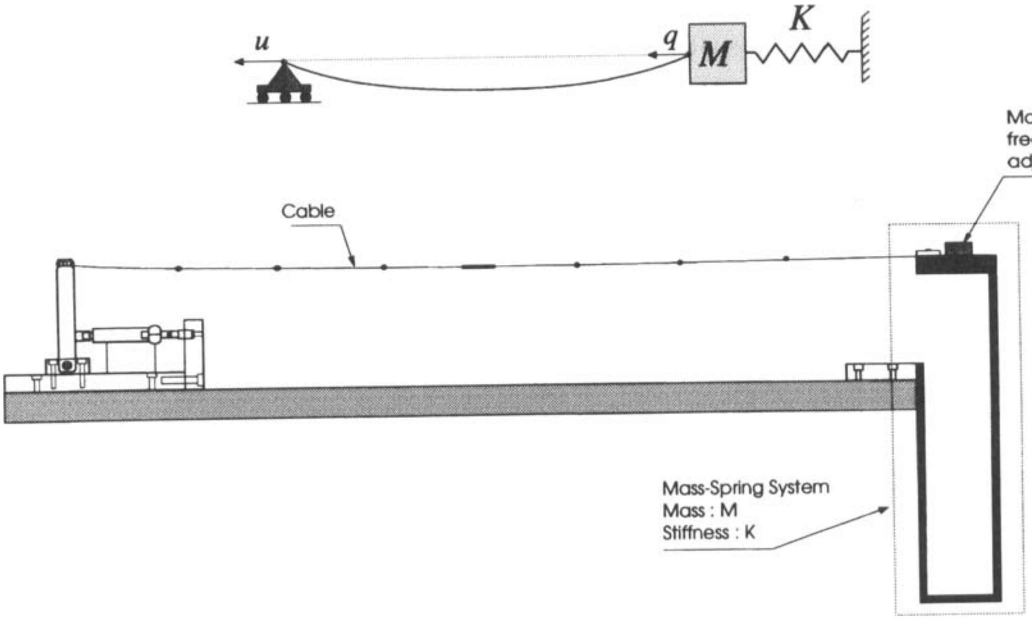

Figure 8. Model of the cable-structure system

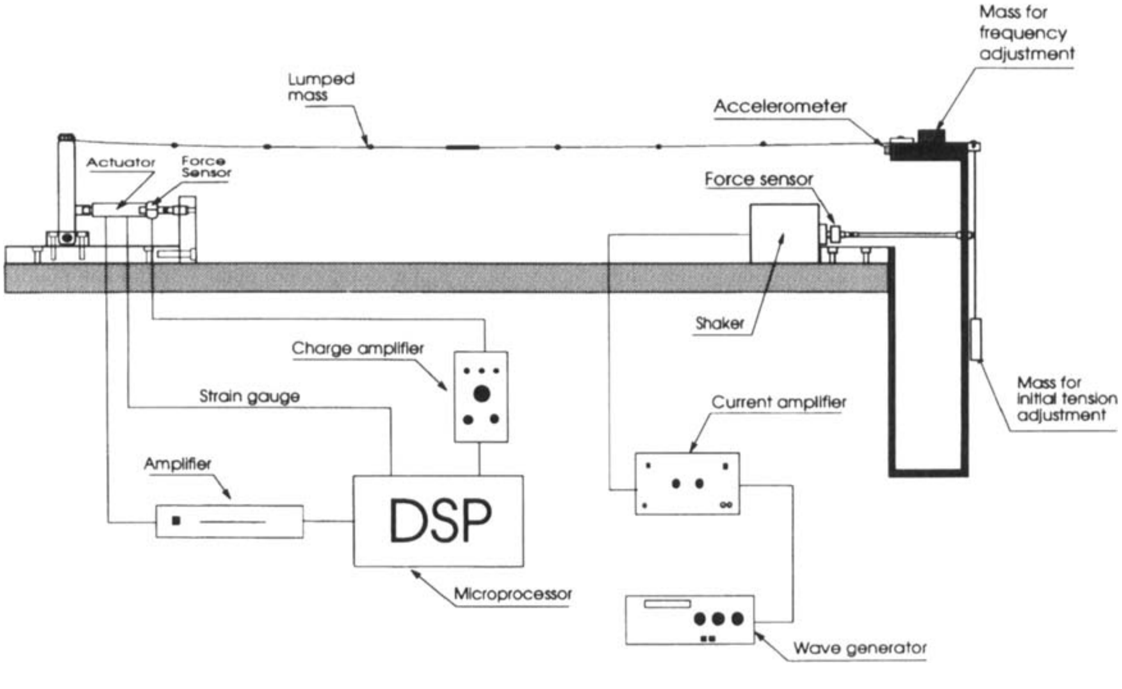

Figure 9. Cable-structure system experimental set-up

4.3. Control law

The proposed control law is, once again, the *Integral Force Feedback* (7). Using the same energy analysis as for the cable alone, it can be shown that the equivalent linear damping introduced by the control in the structure is approximately

$$\xi_{\text{structure}} = \frac{1}{2}\frac{h_u}{K + h_u}\frac{g h_u \omega_q}{\omega_q^2 + (g h_u)^2} \tag{24}$$

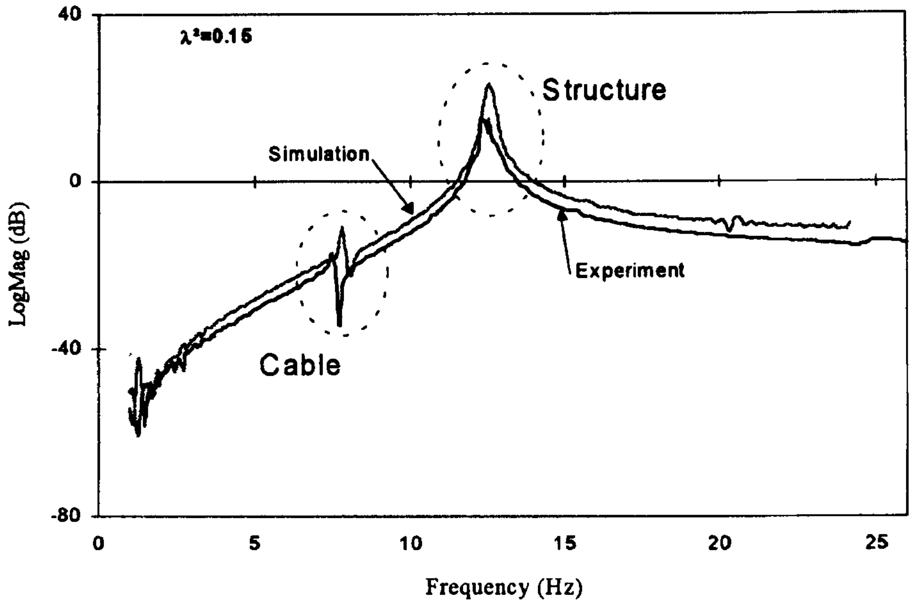

Figure 10. Transfer function between the force applied by the shaker and the acceleration of the mass. Comparison between experiments and simulations.

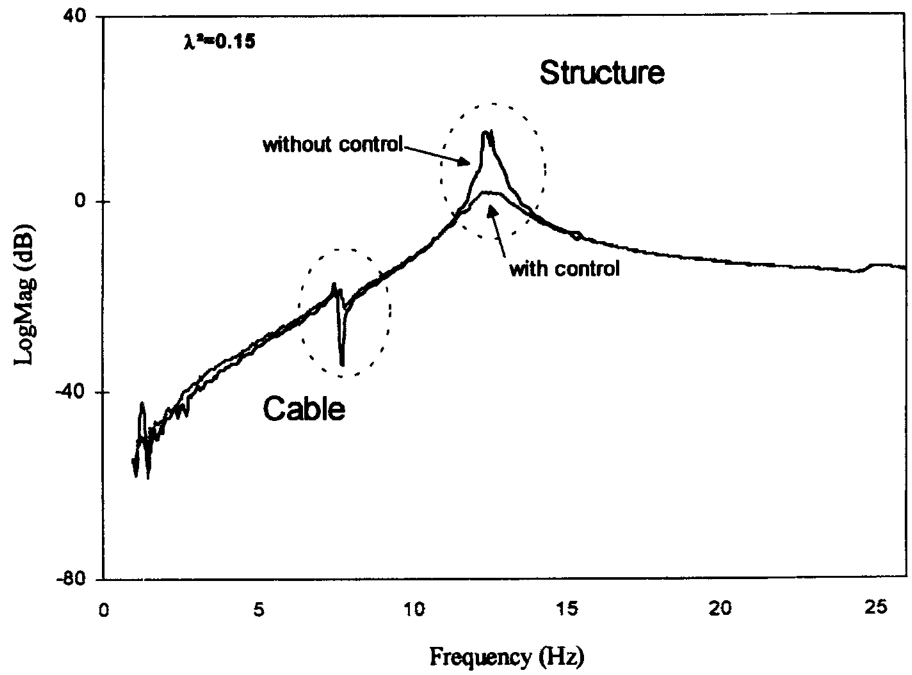

Figure 11. Experimental transfer function between the shaker and the accelerometer with and without control

where h_u is the static stiffness of the cable and K is that of the structure. Equation (24) has been obtained without taking into account the coupling between the structure and cable vibration.

4.4. *Experimental results*

Figure 11 compares the transfer functions with and without control, when $f_{cable} = 8$ Hz, $\lambda^2 = 0{\cdot}15$ and $f_{structure} = 12{\cdot}6$ Hz. The corresponding time-histories of the transient responses are compared in Figure 12.

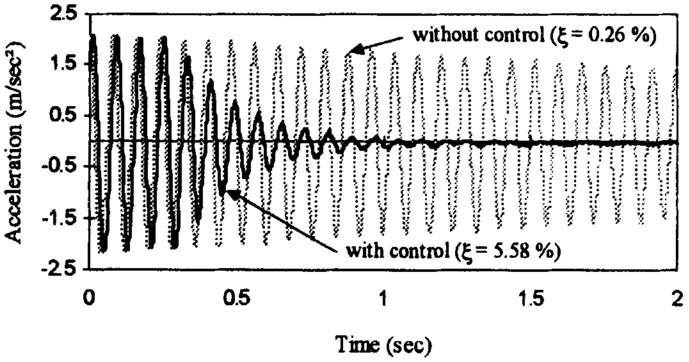

Figure 12. Free response of the structure with and without control

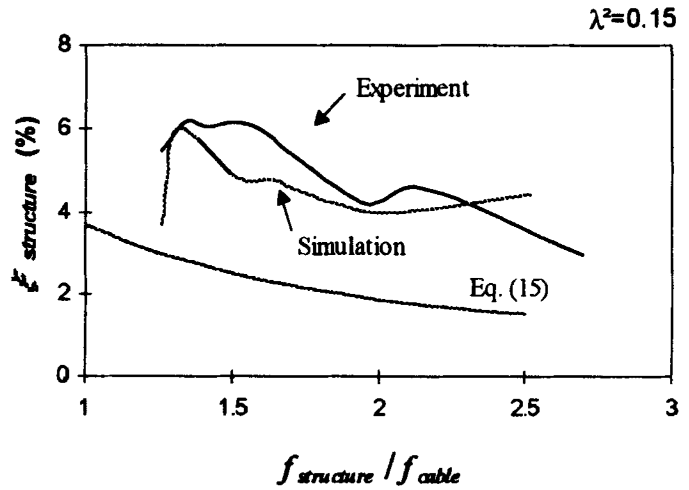

Figure 13. Damping ratio of the global mode

Figure 13 shows the evolution of the active damping with the ratio $f_{\text{structure}}/f_{\text{cable}}$, when the mass M of the structure is changed for fixed values of the cable sag and the control gain g. The figure includes experimental results, simulations obtained from numerical integration of equations (20)–(23) and the approximate formula (24). We notice that the structure remains nicely actively damped at the parametric resonance, when $f_{\text{structure}} = 2f_{\text{cable}}$.

5. CONCLUDING REMARKS

An active tendon consisting of a piezoelectric translator collocated with a force sensor has been developed. It has been shown that the *Integral Force Feedback* enjoys guaranteed stability; and that it produces active damping of the symmetric in-plane modes of the cable, as well as of the coupled cable–structure system. Cable damping is effective even for small sag ($d/l \approx 0{\cdot}5$ percent). The experimental results, $\xi_{\text{cable}} \approx 0{\cdot}018$ for the cable alone, $\xi_{\text{structure}} \approx 0{\cdot}04$–$0{\cdot}06$ for the structure, are superior to previously published results.

In the future, we intend to extend the foregoing approach to the decentralized control of a cable–structure system involving several cables. The present active damping scheme can also be used as *LAC* loop in a *HAC*/*LAC* (High Authority Control/Low Authority Control) strategy for flutter control.

REFERENCES

1. A. H. Nayfeh and D. T. Mook, *Non Linear Oscillations*, Wiley, New York, 1979.
2. B. M. Pacheco, Y. Fujino and A. Sulekh, 'Estimation curve for modal damping in stay cables with viscous damper', *J. struct. eng. ASCE* **119**, 1961–1979 (1993).
3. J. N. Yang and F. Giannopoulos, 'Active control and stability of cable-stayed bridge', *J. eng. mech. div. ASCE* **105**, 677–694 (1979).
4. J. N. Yang and F. Giannopoulos, 'Active control of two-cable-stayed bridge', *J. eng. mech. div. ASCE* **105**, 795–810 (1979).
5. P. Warnitchai, Y. Fujino, B. M. Pacheco and R. Agret, 'An experimental study on active tendon control of cable-stayed bridges', *Earthquake eng. struct. dyn.* **22**, 93–111 (1993).
6. Y. Fujino and T. Susumpow, 'An experimental study on active control of planar cable vibration by axial support motion', *Earthquake eng. struct. dyn.* **23**, 1283–1297 (1994).
7. J.-C. Chen, 'Response of large space structures with stiffness control', *AIAA j. spacecraft* **21**(5), 463–467 (1984).
8. Y. Fujino, P. Warnitchai and B. M. Pacheco, 'Active stiffness control of cable vibration', *J. appl. mech. ASME* **60**, 948–953 (1993).
9. M. J. Balas, 'Active control of flexible systems', *J. optim. theory appl.* **25**(3), 415–436 (1978).
10. R. H. Cannon and D. E. Rosenthal, 'Experiment in control of flexible structures with noncollocated sensors and actuators', *AIAA j. guidance* **7**(5), 546–553 (1984).
11. R. J. Benhabib, R. P. Iwens and R. L. Jackson, 'Stability of large space structures control systems using positivity concepts', *AIAA j. guidance* **4**(5), 487–494 (1981).
12. A. Preumont, J. P. Dufour and Ch. Malekian, 'Active damping by a local force feedback with piezoelectric actuators', *AIAA j. guidance* **15**(2), 390–395 (1992).
13. H. M. Irvine, *Cable structures*, M. I. T. Press, Cambridge, Mass. (1981).